Research article

polymers advanced technologies

Received: 16 March 2010, Revised: 11 October 2010, Accepted: 10 November 2010, Published online in Wiley Online Library: 27 February 2011

(wileyonlinelibrary.com) DOI: 10.1002/pat.1899

Characterization and antibacterial activity of chitosan-based composites with polyester

Chin-San Wu[a]*

The effects of replacing poly(butylene succinate adipate) (PBSA) with acrylic acid-grafted PBSA (PBSA-g-AA) on the structure and the properties of a PBSA/chitosan composite were investigated. The properties of both PBSA-g-AA/chitosan and PBSA/chitosan were compared using Fourier transform infrared (FTIR), ^{13}C nuclear magnetic resonance (NMR), X-ray diffraction (XRD), and an antibacterial activity test. With PBSA-g-AA in the composite, the compatibility with chitosan and, consequently, the properties of the composite became greatly improved due to the formation of ester and imide groups that conferred better dispersion and homogeneity of chitosan in the matrix. Composites containing PBSA-g-AA/chitosan exhibited superior mechanical properties due to greater compatibility between the two components. Moreover, chitosan enhanced the antibacterial activity of the composites. Composites of PBSA-g-AA or PBSA that contain chitosan have better antibacterial activity. The functionalized PBSA-g-AA/chitosan composites showed markedly enhanced antibacterial properties due to the carboxyl groups of acrylic acid, which acted as coordination sites for the chitosan phase, allowing the formation of stronger chemical bonds. Copyright © 2011 John Wiley & Sons, Ltd.

Keywords: composites; PBSA-g-AA/chitosan; antibacterial activity

INTRODUCTION

Among commercialized biodegradable plastics, artificial biodegradable polyesters are still based mainly on industrial plastics such as polylactide (PLA), polycaprolactone (PCL), poly(3-hydroxybutyric acid-co-3-hydroxyvaleric acid) (PHBV), and Poly(butylene succinate adipate) (PBSA). Conventional biodegradable polyesters have already found commercially successful applications in implants, blood bags, packaging, and degradable films.[1–4] Poly(butylene succinate adipate) (PBSA) is a biodegradable and biocompatible polyester. PBSA can be used for biomedical applications because of its biocompatibility and non-toxicity.[5] Some plastics are recyclable, but most are irrecoverable and end up in landfill burial sites. Not only is it increasingly difficult to find such sites, many environmental problems are associated with this method of plastics disposal. For these reasons, it has become important to develop biodegradable polymers for use in plastics. One such polymer, poly(butylene succinate adipate) (PBSA) has received a great deal of attention due to its mechanical strength, hydrophobic nature, and biodegradability.[6,7] However, high production costs appear to limit its commercial applications. This limitation can be overcome by blending PBSA with cost-effective, biodegradable, natural biopolymers such as starch, cellulose, chitosan, or natural fibers to create new materials with improved physical properties,[8–11] and interest in the production of biodegradable polymers using these renewable resources is now growing.[12]

Chitosan (CS) is a widely used natural, abundant biopolymer that is produced commercially from crustacean (shrimp and crabs) waste shell processing; it can also be obtained from the chitin component of fungal cell walls. In addition to being derived from renewable resources, chitosan offers unique physical, chemical, and biological properties, which have been studied for various applications.[13] Chitosan is a polysaccharide well-known for its numerous and interesting biological properties. Indeed, it is a biocompatible, bioresorbable, antibacterial, and bioactive biopolymer. It has been used as a wound healing accelerator, as a health food to reduce blood cholesterol levels, and an immune system stimulant.[14,15] One such feature, the high content of primary amino groups, confers two important characteristics to this biopolymer. First, because the amino groups are basic, it can be protonated at moderately low pH (<6.3) and the resultant cationic polyelectrolyte is water-soluble. Second, the nucleophilicity of the amino groups means that they are deprotonated at higher pH values (>7), and the unshared electron pair can undergo a variety of reactions. The reactivity of these amino groups allows the chemical modification of chitosan under mild conditions, and because of the mild conditions, such modification is typically confined to its amino groups.[16,17] This suggests good potential for controlled modification of the functional properties of chitosan.

Despite the apparent advantages of PBSA/chitosan blends, their utility is limited because of their susceptibility to water absorption and their inferior mechanical properties caused by poor adhesion between the hydrophobic PBSA polymer and the hydrophilic chitosan biopolymer. Adhesion of the two polymers can be aided by using a compatibilizer to improve the

* *Correspondence to: C.-S. Wu, Department of Chemical and Biochemical Engineering, Kao Yuan University, Kaohsiung County, Taiwan 82101, Republic of China.*
E-mail: cws1222@cc.kyu.edu.tw

a *C.-S. Wu*
Department of Chemical and Biochemical Engineering, Kao Yuan University, Kaohsiung County, Taiwan 82101, Republic of China

compatibility between the two immiscible phases, thereby improving the mechanical properties of the composite.[18] Wu[19] used acrylic acid as a compatibilizer grafted onto polylactide and demonstrated increased compatibility between the polylactide and starch. This suggests that grafting a reactive functional group onto PBSA in a PBSA/chitosan blend is likely to produce a blend that offers the best combination of low cost and good mechanical properties.

In this study, the effect of grafting acrylic acid onto PBSA in a PBSA/chitosan blend on the structure and antibacterial properties of the blend was investigated. The composites were characterized using FTIR spectroscopy, ^{13}C nuclear magnetic resonance, and X-ray diffraction (XRD) to identify the structural changes caused by the grafting of acrylic acid. To our knowledge, chitosan has not been systematically evaluated previously as a reinforcement material in PBSA for the production of antibacterial composites.

EXPERIMENTAL

Materials

Poly(butylene succinate adipate) was supplied by Mitsubishi Chemical Co., Ltd (Tokyo, Japan). Acrylic acid (AA), supplied by Sigma-Aldrich (St. Louis, MO), was purified by recrystallization with chloroform before use. PBSA-g-AA was synthesized from these constituents in our laboratory. Benzoyl peroxide (BPO), the initiator in the grafting reaction, was purified by dissolving in chloroform and reprecipitating it with methanol. Chitosan (degree of deacetylation 83.8%), supplied by Tokyo Kasei Kogyo Co. Ltd (Tokyo, Japan), was purified before use; it was first dissolved in 1% acetic acid solution and then precipitated by the addition of 1 M NaOH solution. The precipitate was washed several times with deionized water until it became neutral.

Sample preparation

Graft reaction and sample preparation

A mixture of AA and BPO was added in four equal portions at 2-min intervals to molten PBSA to allow grafting to take place. The reactions were carried out under a nitrogen atmosphere at $85 \pm 2^{\circ}C$. Preliminary experiments showed that reaction equilibrium was attained in less than 6 hr; thus, reactions were allowed to progress for 6 hr at a rotor speed of 60 rpm. The product was dissolved in refluxing xylene (4 g in 200 ml) at $85 \pm 2^{\circ}C$ and the solution was then filtered through several layers of cheesecloth. The xylene-insoluble product remaining on the cheesecloth was washed using acetone to remove the unreacted acrylic acid and then dried in a vacuum oven at 80°C for 24 hr. The xylene-soluble product in the filtrate was extracted five times using 600 ml of cold acetone for each extraction. The subsequent grafting percentage was about 6.86 wt% by titration.[20] BPO and AA loadings were maintained at 0.3 and 10 wt%, respectively.

Composite preparation

The chitosan was dried in an oven at 50°C for 3 days prior to composite preparation. The mass ratios of chitosan to PBSA were fixed at 5/95, 10/90, 15/85, and 20/80, and composites were prepared using a "Plastograph" 200 Nm mixer W50EHT instrument (Brabender, Hackensack, NJ) with a blade-type rotor; the rotor speed was maintained at 50 rpm and the temperature at 100°C, with a reaction time of 15 min. Next, the composites were pressed into 1-mm-thick plates using a hot press at 100°C, and then placed in a desiccator for cooling. The cooled plates were then made into standard samples for characterization.

NMR/FTIR/XRD analyses

Solid-state ^{13}C NMR was performed using an AMX-400 NMR spectrometer (Bruker, Billerica, MA) and was obtained at 100 MHz under cross-polarization while spinning at the magic angle. Power decoupling conditions were set with a 90° pulse and a 4 sec cycle time. Infrared spectra of the samples were obtained using an FTS-7PC FTIR spectrophotometer (Bio-Rad, Hercules, CA). X-ray diffraction (XRD) data were recorded using a 3 V X-ray diffractometer (Rigaku, Tokyo, Japan) with a Cu target and a K_{α} source at a scanning rate of 2°/min.

Composite morphology

A thin film of each composite was created using a hydrolytic press and treated with hot water at 80°C for 24 hr before being coated with gold. The surface morphology of these thin films was observed using a scanning electron microscope (SEM; model S-1400, Hitachi Microscopy, Tokyo, Japan).

Determination of antibacterial properties

Escherichia coli, which is used widely as a biological index for pollution and contamination in water and instrumentation, was chosen as the standard bacterium for determining the antibacterial properties of the composite materials. *E. coli* (BCRC 10239) was obtained from the Bioresource Collection and Research Center (BCRC; Hsinchu, Taiwan) and was maintained in nutrient broth (NB) medium (3 g beef extract and 5 g peptone in 1 L of distilled water, pH 7.0). Nutrient agar was produced with the addition of 15 g of agar to 1 L of NB. The bacteria were stored at –20°C in NB medium containing 60% glycerol. Prior to testing, 150 ml of NB medium was inoculated with 10 μl of preserved bacteria, and the culture was grown aerobically at 35°C. After overnight incubation, 3 ml of the culture was transferred to fresh NB medium and incubated at 35°C with shaking at 120 rpm for 18 hr. A well was constructed (3.00 cm diameter and 0.03 cm thick) on the surface of each sample (5.00 cm diameter and 0.10 cm thickness) to hold the bacterial suspension in contact with the composite sample. A 0.02-ml aliquot of bacterial suspension ($1.3 \pm 0.3 \times 10^6$ colony-forming units [CFUs]/ml) was placed on the surface of each sample and covered with a germless polyethylene film (4.00 cm diameter and 0.05 cm thick; Fig. 1). The samples were incubated at $35 \pm 1^{\circ}C$ at a relative humidity of approximately 90%. After incubation, samples were washed with 1.98 ml of NaCl solution (0.85%) for 3–24 hr. The washing solution was diluted by 10^5 with NaCl solution, and the number of CFUs of *E. coli* was determined by direct plate counting.

Analysis of antibacterial capacity

The survival ratio of bacteria exposed to the composite material was used to determine the antibacterial capacity of PBSA or

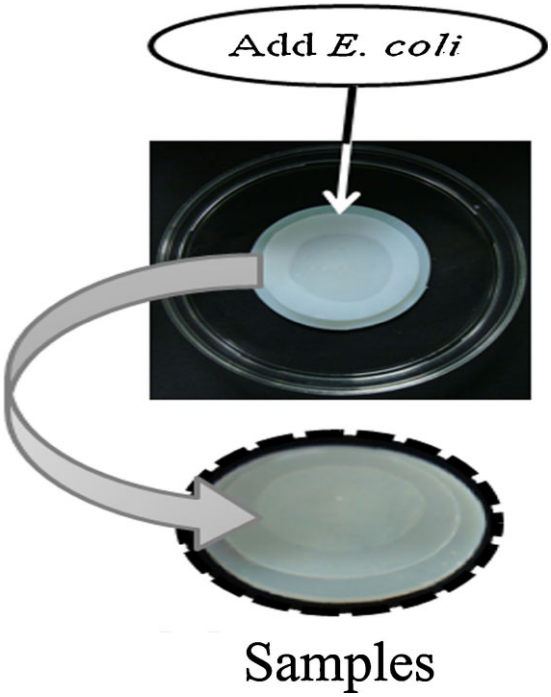

Figure 1. Photographs of samples of PBSA and its composites loaded with a fixed volume (0.1 ml) of *E. coli*. This figure is available in color online at wileyonlinelibrary.com/journal/pat

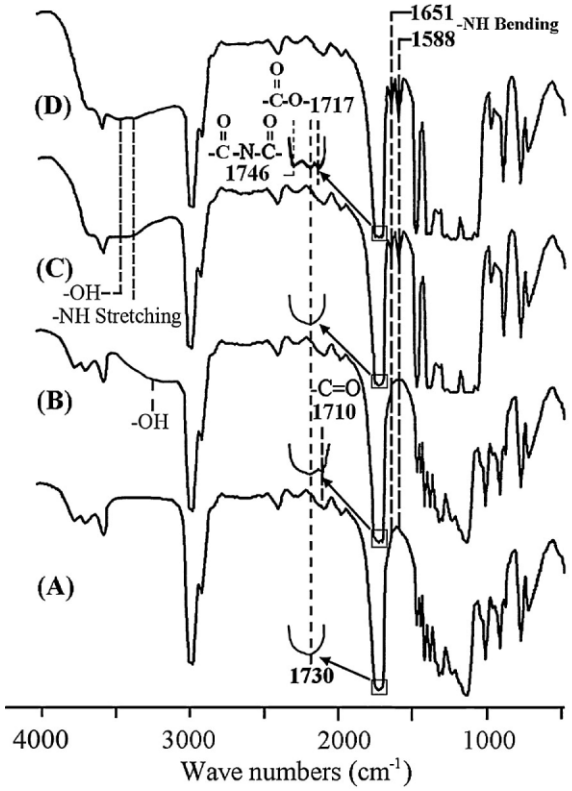

Figure 2. FTIR spectra of (A) PBSA, (B) PBSA-g-AA, (C) PBSA/chitosan (10 wt%), and (D) PBSA-g-AA/chitosan (10 wt%).

PBSA-g-AA and their composites. The survival ratio of bacteria was defined by the following equation:

$$\text{Survival ratio} = \frac{y}{x} \times 100\%, \quad (1)$$

where x and y are the CFU counts before and after exposure. The survival ratio of *E. coli* was calculated using eqn (3). Almost no *E. coli* survived.

JISL 1902–1998, a method used typically to estimate drug toxicity, can also be applied to determining the antibacterial activity of chitosan composites. This method determines an antibacterial index (ABI) and kill-bacterial index (KBI) according to the following expressions:

$$\text{ABI} = \log B - \log C \quad (2)$$

$$\text{KBI} = \log A - \log C \quad (3)$$

where A is the number of bacteria recovered from the inoculated, untreated sample (native PBSA or PBSA-g-AA) immediately following inoculation; B is the number of bacteria remaining in the inoculated, untreated sample after 18 hr; and C is number of bacteria remaining in the inoculated, treated sample after 18 hr. According to the antibacterial standard of the Japanese Association for the Functional Evaluation of Textiles, an ABI value greater than 2.2 indicates bacterial inhibition, and a KBI value greater than 0 indicates a bactericidal effect.

RESULTS AND DISCUSSION

FTIR/NMR analyses

The grafting of AA onto PBSA was analyzed by FTIR. Figure 2(A) and (B) show the FTIR spectra of PBSA and PBSA-g-AA. In addition to the characteristic peaks (3300–3700, 1700–1760, and 500–1500 cm^{-1}) observed with both polymers, there exists an obvious extra peak at 1710 cm^{-1} for the modified PBSA, which is characteristic of –C=O and represents the free acid in the modified polymer. This peak at 1710 cm^{-1}, as well as a broad –OH stretching absorbance at 3200–3700 cm^{-1}, also reported elsewhere,[20,21] demonstrates that AA had been grafted onto PBSA.

Furthermore, the FTIR spectra of PBSA/chitosan (10 wt%) (Fig. 2C) and PBSA-g-AA/chitosan (10 wt%) (Fig. 2D) show peaks between 3200 and 3700 cm^{-1} that are much more intense than the stretching absorbance at 3000–3600 cm^{-1} observed in the absence of chitosan (Fig. 2). In the spectrum, chitosan exhibited peaks at 3300–3650 cm^{-1}, which are assigned to the –NH and hydrogen bonded –OH stretch vibrational frequencies, while a peak at 3450 cm^{-1} is that of free –OH bond stretch of glucopyranose units.[22] The spectra of PBSA-g-AA/chitosan (10 wt%) show additional unique absorption peaks at 1717 and 1746 cm^{-1}. The peak at 1717 cm^{-1} is assigned to –C=O of $N(COR)_2$ while the peaks at 1746 cm^{-1} are assigned to absorption of –C=O in OCOR. These ester and imide functional groups are formed via the reaction between –OH of PBSA-g-AA and –NH of chitosan when the two polymers are blended. Zong *et al.*[23] studied acylated chitosan copolymers, with similar results. Additionally, the spectra in Fig. 2 identify differences in absorbance intensity at 1651 cm^{-1} (amide I, secondary amide) and 1588 cm^{-1} (nonacylated primary amide). The absorbance at 1588 cm^{-1} in PBSA/chitosan is much greater than at 1651 cm^{-1}, while it is less marked in PBSA-g-AA/chitosan. This result, similar to that obtained by Nge *et al.*,[24] indicates that in the blending of PBSA-g-AA with chitosan, part of the primary amide of chitosan reacts with the carboxyl group of PBSA-g-AA.

To further confirm the grafting of AA, the structures of PBSA and PBSA-g AA were compared using solid-state ^{13}C NMR. The spectrum for unmodified PBSA shows six carbon peaks (1, 2: $\delta = 24.5$ ppm; 3: $\delta = 28.7$ ppm; 4: $\delta = 33.6$ ppm; 5: $\delta = 63.2$ ppm; 6: $\delta = 171.3$ ppm; 7: $\delta = 172.8$ ppm; Fig. 3A), an outcome also reported by Ahn *et al.*[25] in their study on the synthesis of biodegradable copolymers from succinic acid and adipic acid with 1,4-butanediol. Three extra peaks in the spectrum of PBSA-g-AA (8: $\delta = 42.2$ ppm; 9: $\delta = 36.2$ ppm; 10: –C=O $\delta = 175.1$ ppm; Fig. 3B) confirm the grafting of AA onto PBSA.

The solid-state ^{13}C NMR spectra of PBSA-g-AA/chitosan (10 wt%), PBSA/chitosan (10 wt%) and original chitosan are shown in Fig. 3(D and E), respectively. The spectrum of original chitosan is the same as that reported by Zong *et al.*[23] Moreover, the PBSA-g-AA/chitosan (10 wt%) spectrum coincides with the solid-state ^{13}C NMR results for acylated chitosan by Zong *et al.*[23] Comparing the spectra of PBSA/chitosan (10 wt%) and PBSA-g-AA/chitosan (10 wt%), we found extra peaks at $\delta = 42.2$ ppm (C_α) and $\delta = 36.2$ ppm (C_β) in the latter. These peaks were also observed in our previous report[19] on solid-state ^{13}C NMR of PBSA-g-AA/chitosan. As indicated, the appearance of peaks at C_α and C_β in PBSA-g-AA is due to the grafting of AA onto PBSA. However, the peak at $\delta = 175.1$ ppm (C=O) shown in Fig. 3(B) that also characterizes the grafting of AA onto PBSA is absent in the solid-state spectrum of PBSA-g-AA/chitosan (10 wt%; Fig. 3C). This is because the reaction between –COOH of AA and –OH or –NH of chitosan shifted the peak at $\delta = 175.1$ ppm to the duplicates at 11, 12, 13, 14, and 15 ($\delta = 178.5$, 177.3, 171.3, 169.8, and 168.5 ppm). This is evidence of a condensation reaction between PBSA-g-AA and chitosan, through which the original chitosan was fully acylated and the amino and amide groups were converted to imides (represented by peaks 13, 14, and 15 in Fig. 3C). This reaction does not occur between PBSA and chitosan, a point illustrated by the absence of corresponding peaks in the PBSA/chitosan (10 wt%) spectrum (Fig. 3D). The formation of imide and ester functional groups noticeably affected the thermal, mechanical, and biodegradation properties of PBSA-g-AA/chitosan.

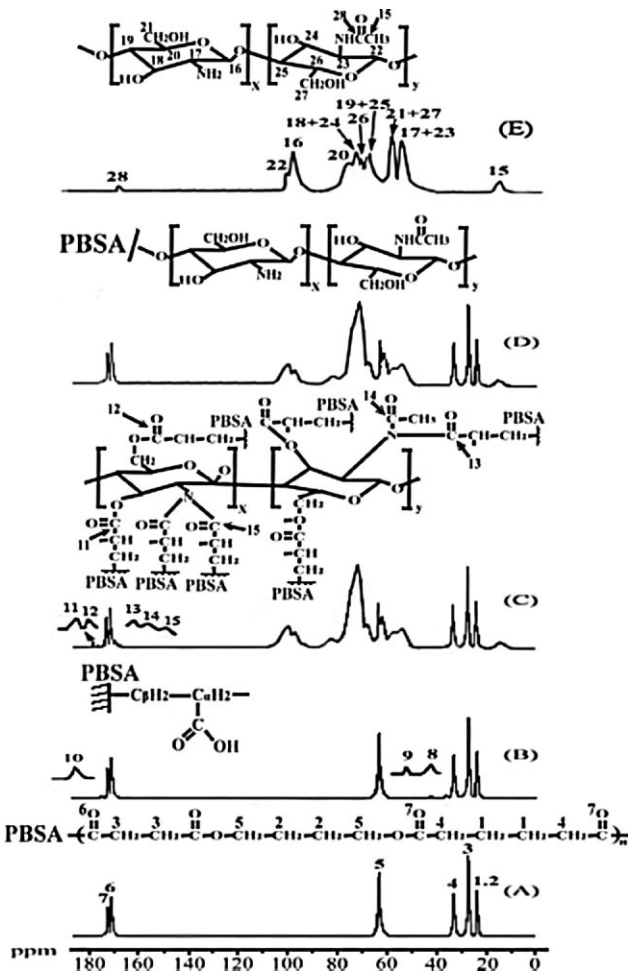

Figure 3. Solid-state ^{13}C NMR spectra of (A) PBSA, (B) PBSA-g-AA, (C) PBSA-g-AA/chitosan (10 wt%), (D) PBSA/chitosan (10 wt%), and (E) chitosan.

X-ray diffraction

The X-ray diffraction spectra of pure PBSA, PBSA/chitosan (10 wt%), PBSA-g-AA/chitosan (10 wt%), and pure chitosan are shown in Fig. 4(A–D), respectively. Similar to the results of Ray and Bousmina,[26] pure PBSA (Fig. 4A) exhibited two diffraction peaks at about 19.7° and 22.6°. Chitosan exhibited two diffraction peaks at about 9.6° and 19.5°, as reported by Chen *et al.*[27] The two blends, meanwhile, produced an extra peak at about 9.6° (Fig. 4B and C). This peak was also observed in the spectrum of pure chitosan (Fig. 4D) and is caused by the blending of chitosan with PBSA or PBSA-g-AA. Two peaks, present in the PBSA-g-AA/chitosan spectrum but not in the PBSA/chitosan spectrum at $2\theta = 18.1°$ and the peak at 19.5°, shifted to 19.1°. These differences between the two blends may be due to the generation of ester and imide carbonyl functional groups, as described in the discussion of FTIR and NMR analysis. Muzzarelli

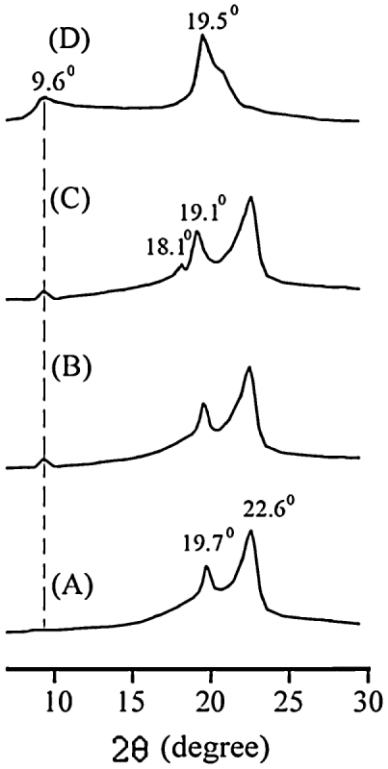

Figure 4. X-ray diffractograms for (A) PBSA, (B) PBSA/chitosan (10 wt%), (C) PBSA-g-AA/chitosan (10 wt%), and (D) chitosan.

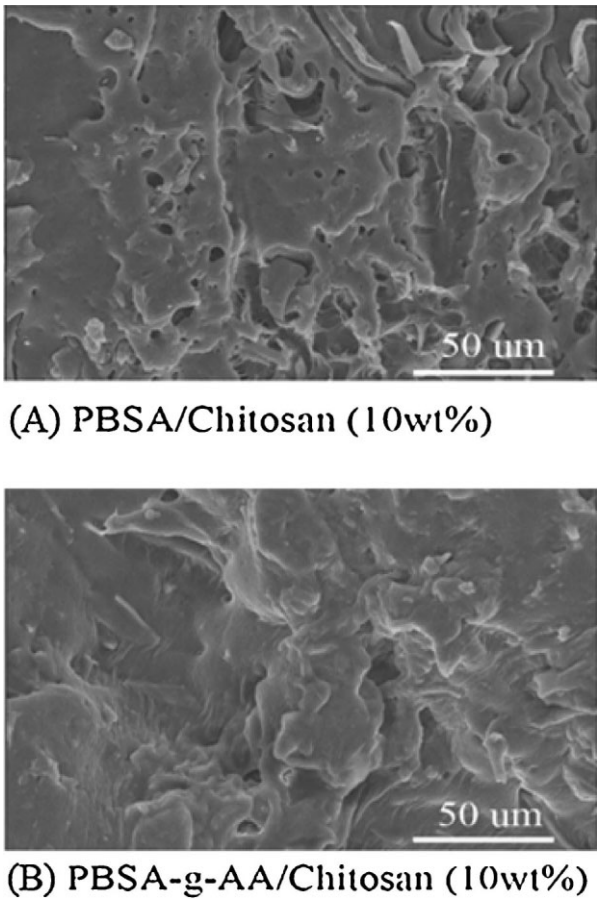

Figure 5. SEM microphotographs showing the distribution and adhesion of chitosan in (A) PBSA/chitosan (10 wt%) and (B) PBSA-g-AA/chitosan (10 wt%) composites.

et al.[28] reported similar results. One can therefore conclude that the crystalline structure of the blend is altered when PBSA-g-AA is used as a compatibilizer in the PBSA/chitosan system.

Composite morphology

In most composite materials, effective wetting and uniform dispersion of all components in a given matrix, and strong interfacial adhesion between the phases are required to obtain a composite with satisfactory mechanical properties. In the current study, chitosan may be thought of as a dispersed phase within a PBSA or PBSA-g-AA matrix. To evaluate the composite morphology, SEM was employed to examine tensile fractures in the surfaces of PBSA/chitosan (10 wt%) and PBSA-g-AA/chitosan (10 wt%) samples. The SEM microphotograph of PBSA/chitosan (10 wt%) in Fig. 5(A) shows that the chitosan fibers in this composite tended to agglomerate into bundles and were distributed unevenly in the matrix. This poor dispersion was due to the formation of hydrogen bonds between chitosan and the disparate hydrophilicities of PBSA and chitosan. Poor wetting in these composites was also noted (Fig. 5A) due to large differences in surface energy between the chitosan and the PBSA matrix.[9]

In contrast, the PBSA-g-AA/chitosan (10 wt%) microphotograph presented in Fig. 5(B) shows a more homogeneous dispersion and better wetting of chitosan in the PBSA-g-AA matrix, as indicated by the complete coverage of PBSA-g-AA on the fiber and the removal of both materials when a fiber was pulled from the bulk. This improved interfacial adhesion is due to the similar hydrophilicity of the two components, which allows for the formation of branched and cross-linked macromolecules, and the prevention of hydrogen bonding between chitosan fibers.

Mechanical properties

Figure 6 illustrates the variations in tensile strength and elongation at breaking with chitosan content for PBSA/chitosan and PBSA-g-AA/chitosan composites. The tensile strength and elongation of pure PBSA decreased after grafting with acrylic acid. For PBSA/chitosan composites (Fig. 6A), the tensile strength decreased markedly and continuously with increasing chitosan content. This is attributable to the poor dispersion of chitosan in the PBSA matrix, as discussed above (Fig. 5A). The effect of this incompatibility on the mechanical properties of the composites is substantial. The PBSA-g-AA/chitosan composites in Fig. 6(A) exhibited a unique behavior with regard to the tensile strength at breaking, which increased with increasing chitosan content despite the fact that PBSA-g-AA had a lower tensile strength than the pure PBSA. Furthermore, the tensile strength of the PBSA-g-AA/chitosan composites was constant with chitosan

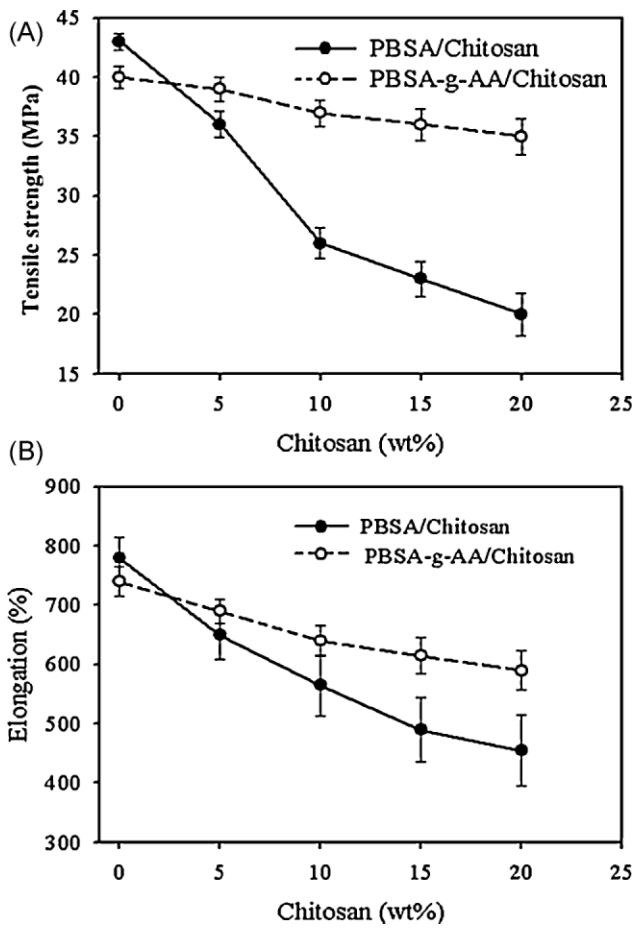

Figure 6. Effect of chitosan content on (A) tensile strength and (B) elongation at break for PBSA/chitosan and PBSA-g-AA/chitosan composites.

Table 1. Effect of chitosan content on the antibacterial properties of PBSA/chitosan and PBSA-g-AA/chitosan composites

	PBSA/chitosan			PBSA-g-AA/chitosan		
	5 wt%	10 wt%	20 wt%	5 wt%	10 wt%	20 wt%
A	1.31×10^6	1.31×10^6	1.31×10^6	1.31×10^6	1.31×10^6	1.31×10^6
B	2.19×10^8	2.19×10^8	2.19×10^8	1.06×10^8	1.06×10^8	1.06×10^8
C	8.01×10^3	0	0	3.01×10^3	0	0
ABI	4.43	>8.33	>8.33	4.54	>8.02	>8.02
KBI	2.21	>6.11	>6.11	2.63	>6.11	>6.11

content beyond 10 wt%. This behavior is likely due to an enhanced dispersion of chitosan in the PBSA-g-AA matrix resulting from the formation of branched or cross-linked macromolecules.

Figure 6(B) also indicates less elongation at break values for the PBSA/chitosan composites relative to the PBSA-g-AA/chitosan composites. In PBSA/chitosan, the chitosan tended to agglomerate into bundles, illustrating the poor compatibility between the two phases. In the PBSA-g-AA/chitosan composites, as shown by the solid line in Fig. 6(B), the elongation at break also decreased with increasing amounts of chitosan, but exhibited greater elongation values than PBSA/chitosan composites. However, these values are still lower than those of pure PBSA. These results are similar to those of Wu.[29] The data in Fig. 6 indicate that the grafting reaction in PBSA-g-AA/chitosan composites improves the tensile strength and elongation of PBSA/chitosan. However, the degree of enhancement in elongation is less than that in tensile strength.

Antibacterial properties of composites

Antibacterial activity was evaluated with clinical infectious *E. coli*. ABI and KBI values were calculated according to JISL 1902–1998 and are presented in Table 1. As shown in Fig. 7, the *E. coli* cell count increased with time from 1.31×10^6 to 1.29×10^8 CFU ml^{-1} or from 1.31×10^6 to 1.06×10^8 CFU ml^{-1}, respectively, after incubation at 37°C for 24 hr, when in contact with PBSA or PBSA-g-AA. Conversely, under the same conditions, the bacterial cell count decreased rapidly to near zero when in contact with PBSA/chitosan or PBSA-g-AA/chitosan containing more than 10 wt% chitosan. At 10 wt% chitosan, the onset of *E. coli* reduction was observed at 6 hr. From the results in Table 1 and the guidelines set forth by JISL 1902–1998 and the Japanese Association for the Functional Evaluation of Textiles, one can conclude that PBSA-g-AA/chitosan suppresses the growth of *E. coli*. All of the samples of PBSA-g-AA/chitosan exhibited a higher degree of bacterial suppression than the corresponding samples of PBSA/chitosan. This is a result of the formation of ester and imide carbonyl functional groups from the condensation of the carboxylic acid groups of PBSA-g-AA with part of the primary amide and hydroxyl groups of chitosan.

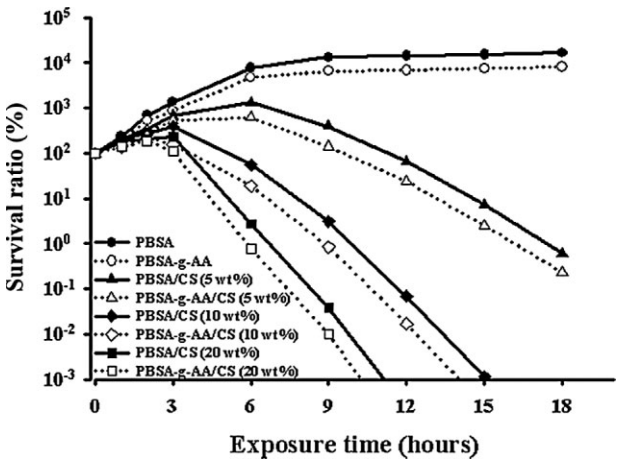

Figure 7. Exposure time course for survival ratio of *E. coli* cells during exposure to PBSA or PBSA-g-AA and their composite surfaces.

Figure 7 demonstrates that the survival ratio of *E. coli* in contact with PBSA or PBSA-g-AA increased with time up to 12 hr, when equilibrium was reached. In contrast, the survival ratio of *E. coli* in contact with PBSA/chitosan or PBSA-g-AA/chitosan began to decrease after only 6 hr. Thus, composite materials with chitosan suppressed the growth of *E. coli*. Composites containing more than 10 wt% chitosan showed a rapid decrease in the survival ratio in the first 18 hr and a slower decline thereafter. The survival ratio for both PBSA/chitosan and PBSA-g-AA/chitosan, which inversely indicates the extent of antibacterial activity, decreased as the content of chitosan increased. Consistently, the PBSA-g-AA/chitosan composites yielded a lower survival ratio than the PBSA/chitosan composites. The higher antibacterial activity of PBSA-g-AA/chitosan may be a result of the formation of ester and imide carbonyl functional groups from PBSA-g-AA and chitosan. Bacterial strains, such as *E. coli*, with an extracellular capsule, carry less negative charge and are less prone to adsorption on the positively charged surface of PBSA-g-AA/chitosan. However, the composites of PBSA/chitosan or PBSA-g-AA/chitosan have better antibacterial activity.

CONCLUSIONS

The compatibility and mechanical properties of a PBSA/chitosan composite were improved by using PBSA-g-AA in place of PBSA. The blending of PBSA-g-AA with chitosan leads to the formation of ester carbonyl and amide functional groups that are not present in PBSA/chitosan. These groups are responsible for many of the differences in mechanical properties between the two copolymers. Although tensile strength and elongation at break worsened in both composites with increasing chitosan content, the deterioration was not so marked for PBSA-g-AA/chitosan. Antibacterial activity was enhanced with the addition of 10 wt% chitosan to PBSA-g-AA or PBSA, resulting in ABI and KBI values of more than 8.00 and 6.00, respectively. The antibacterial and

mechanical properties of PBSA-g-AA/chitosan were higher than that of PBSA/chitosan. Thus, the current study demonstrates an enhancement in the compatibility between PBSA and chitosan, with antibacterial and mechanical properties.

REFERENCES

[1] S. Ramakrishna, J. Mayer, E. Wintermantel, W. Leong Kam, *Comp. Sci. Tech.* **2001**, *61*, 1189–1224.
[2] D. G. Yu, W. C. Lin, C. H. Lin, M. C. Yang, *Macromol. Biosci.* **2006**, *6*, 348–357.
[3] G. Kale, R. Auras, S. P. Singh, *Packag. Technol. Sci.* **2007**, *20*, 49–70.
[4] S. Venkatraman, F. Boey, L. L. Lao, *Prog. Polym. Sci.* **2008**, *33*, 853–874.
[5] A. A. Shah, F. Hasan, A. Hameed, S. Ahmed, *Biotechnol. Adv.* **2008**, *26*, 246–265.
[6] J. H. Zhao, X. Q. Wang, J. Zeng, G. Yang, F. H. Shi, Q. Yan, *Polym. Degrad. Stab.* **2005**, *90*, 173–179.
[7] H. Uchida, T. Nakajima-Kambe, Y. Shigeno-Akutsu, N. Nomura, Y. Tokiwa, T. Nakahara, *FEMS Microbiol. Lett.* **2000**, *189*, 125–129.
[8] J. A. Rattoa, P. J. Stenhousea, M. Auerbacha, J. Mitchellb, *Polymer* **1999**, *40*, 6777–6788.
[9] V. M. Correlo, L. F. Boesel, M. Bhattacharya, J. F. Mano, N. M. Neves, R. L. Reis, *Mater. Sci. Eng. A* **2005**, *403*, 57–68.
[10] M. Wollerdorfer, H. Bade, *Indust. Crops Prod.* **1998**, *8*, 105–112.
[11] C. S. Ha, W. J. Cho, *Prog. Polym. Sci.* **2002**, *27*, 759–809.
[12] L. Yua, K. Deana, L. Li, *Prog. Polym. Sci.* **2006**, *31*, 576–602.
[13] S. Kumar, J. Dutta, P. K. Dutta, *Int. J. Biol. Macromol.* **2009**, *45*, 330–337.
[14] W. C. Lin, D. G. Yu, M. C. Yang, *Colloids Surf. B Biointerf.* **2005**, *44*, 82–92.
[15] S. H. Cha, J. S. Lee, C. B. Song, K. J. Lee, Y. J. Jeon, *Aquaculture* **2008**, *278*, 110–118.
[16] V. K. Mourya, N. N. Inamdar, *React. Funct. Polym.* **2008**, *68*, 1013–1051.
[17] N. M. Alves, J. F. Mano, *Int. J. Biol. Macromol.* **2008**, *43*, 401–414.
[18] L. Yu, K. Dean, Q. Yuan, L. Chen, X. Zhang, *J. Appl. Polym. Sci.* **2007**, *103*, 812–818.
[19] C. S. Wu, *Macromol. Biosci.* **2008**, *8*, 560–567.
[20] C. S. Wu, *J. Appl. Polym. Sci.* **2006**, *102*, 3565–3574.
[21] H. P. Zhao, J. T. Zhu, Z. Y. Fu, X. Q. Feng, Y. Shao, R. T. Ma, *Thin Solid Films* **2009**, *516*, 5659–5663.
[22] S. Sahoo, A. Sasmal, R. Nanda, A. R. Phani, P. L. Nayak, *Carbohydr. Polym.* **2010**, *79*, 106–113.
[23] Z. Zong, Y. Kimura, M. Takahashi, H. Yamane, *Polymer* **2000**, *41*, 899–906.
[24] T. T. Nge, M. Yamaguchi, N. Hori, A. Takemura, H. Ono, *J. Appl. Polym. Sci.* **2002**, *83*, 1025–1035.
[25] B. D. Ahn, S. H. Kim, Y. H. Kim, J. S. Yang, *J. Appl. Polym. Sci.* **2001**, *82*, 2808–2826.
[26] S. S. Ray, M. Bousmina, *Polymer* **2005**, *46*, 12430–12439.
[27] Z. Chen, X. Mo, C. He, H. Wang, *Carbohydr. Polym.* **2008**, *72*, 410–418.
[28] R. A. A. Muzzarelli, M. Terbojevich, C. Muzzarelli, O. Francescangeli, *Carbohydr. Polym.* **2002**, *50*, 69–78.
[29] C. S. Wu, *J. Appl. Polym. Sci.* **2003**, *89*, 2888–2895.

